The expansive effects of concentrated pyritic zones within the Devonian Marcellus Shale Formation of North America

S.E. Hoover and D. Lehmann

Quarterly Journal of Engineering Geology and Hydrogeology 2009; v. 42; p. 157-164
doi:10.1144/1470-9236/07-086

The expansive effects of concentrated pyritic zones within the Devonian Marcellus Shale Formation of North America

S.E. Hoover[1,*] & D. Lehmann[2]

[1]CMT Laboratories, Inc., 2701 Carolean Industrial Drive, State College, PA 16801, USA
[2]Environmental Resources Management, 15810 Park Ten Place, Suite 300, Houston, TX 77084, USA
*Corresponding author (e-mail: shoover@cmtlabs.net)

Abstract: Regressive expansion analysis and chemical modelling are conducted to determine the effect of concentrated pyritic zones within the Marcellus Shale Formation. Although the expansive effects of microscopic pyrite are known, concentrated pyritic zones within these carbonaceous mudstones are studied to determine their potential to expand and damage civil infrastructure. Methods of characterizing the expansion potential of pyritic mudstone are scrutinized in an effort to advance the current state-of-practice for geotechnical and geological investigations. Observational data and modelling reveal that oxidation of the concentrated pyritic zones produces microenvironments within the mudstone matrix that lead to the production of significant quantities of heave-inducing hydrous sulphates such as gypsum. These data signify a need to supplement traditional forms of sulphur testing with detailed studies of pyrite morphology, deposition and oxidation availability within fracture zones as a means of identifying swell potential. Additional laboratory testing, such as modified kinetic oxidation models, is required to further quantify the expansive effects of the concentrated pyritic zones.

Pyrite is found in black, carbonaceous mudstones throughout the world. Expansion associated with oxidation of pyritic mudstone and hydrous sulphate precipitation are documented in areas of the USA such as Tennessee (Long & Williams 1990), Virginia, Ohio (Anon. 1960), West Virginia (Dubbe *et al*. 1984), Pennsylvania (Hoover *et al*. 2004), Missouri and Kansas (Coveney & Parizek 1977). The expansive pyritic mudstone problem is also found in England (Hawkins & Pinches 1987), Norway (Moum & Rosenquist 1959), Canada (Penner & Eden 1972; Tanguay *et al*. 1999) and Sweden (Jangdal 1971). Undocumented cases of structural damage caused by expansion of pyritic mudstone are certainly possible given that the problem is generally not recognized by those in the construction industry and by a significant proportion of geotechnical engineers and geologists, and also because of client confidentiality restricting dissemination of case studies to the geological and geotechnical communities.

Pyrite oxidation can occur as a result of advection of oxic groundwater into a pyritic area, but solubility of O_2 in water is relatively low and therefore the extent of reaction may be limited. Reaction is usually more extensive when gaseous O_2 diffuses into an unsaturated zone. The low pH values cause a variety of minerals to precipitate, including gypsum and numerous ferric hydrosulphates (Appelo & Postma 1993; Hammarstrom *et al.* 2004). Flux of gaseous O_2 can be large, resulting in rapid reaction and producing high sulphate and iron concentrations and pH of two or less where there is limited calcite availability. As pH decreases the solubility of Fe(III) increases, resulting in a high flux of oxidizing Fe^{3+} into adjacent saturated zones (Rimstidt & Newcomb 1993). Microbial oxidation by a host of ubiquitous microbes including *Thiobacillus* spp., *Acidithiobacillus ferrooxidans*, etc. can also increase the reaction rate. Jaynes *et al*. (1984*a*,*b*) reported that prime bacterial activity is at a maximum near pH $\approx$ 3.25. Relative humidity, temperature, surface area and morphology also affect the rate of reaction.

The sulphuric acid produced during the oxidation of pyrite reacts with calcite ($CaCO_3$) to produce gypsum ($CaSO_4.2H_2O$), which involves an expansion in volume (Bell 2000). The calcite can originate within the mudstone matrix, as fracture fillings or from surrounding formations and saturated groundwater. Other hydrous sulphates that are produced from the oxidation of pyrite include melanterite ($FeSO_4.7H_2O$), halotrichite ($FeAl_2(SO_4)_4.22H_2O$), ochre (FeO(OH)) and other base exchange products such as jarosite ($KFe_3(SO_4)_2(OH)_6$).

The evolution of the expansive process is described in Figure 1, which highlights the features in common within case histories where structural damage has resulted from the presence of pyritic mudstone.

Although the understanding of the pyrite oxidation is well documented because of its infamous ability to cause significant environmental problems associated with acid mine drainage (Brady *et al*. 1998) and acid rock drainage (Gold & Doden 2006), there is little in the literature on determining the potential for swelling through the conversion of sulphide to sulphate. Various studies have suggested that the potential for swelling is based solely on the amount of pyritic sulphur, with values greater than 0.1% causing structural damage of civil infrastructure, and there has been minor to no emphasis on oxidation availability and transport mechanisms such as

Quarterly Journal of Engineering Geology and Hydrogeology, **42**, 157–164
DOI 10.1144/1470-9236/07-086

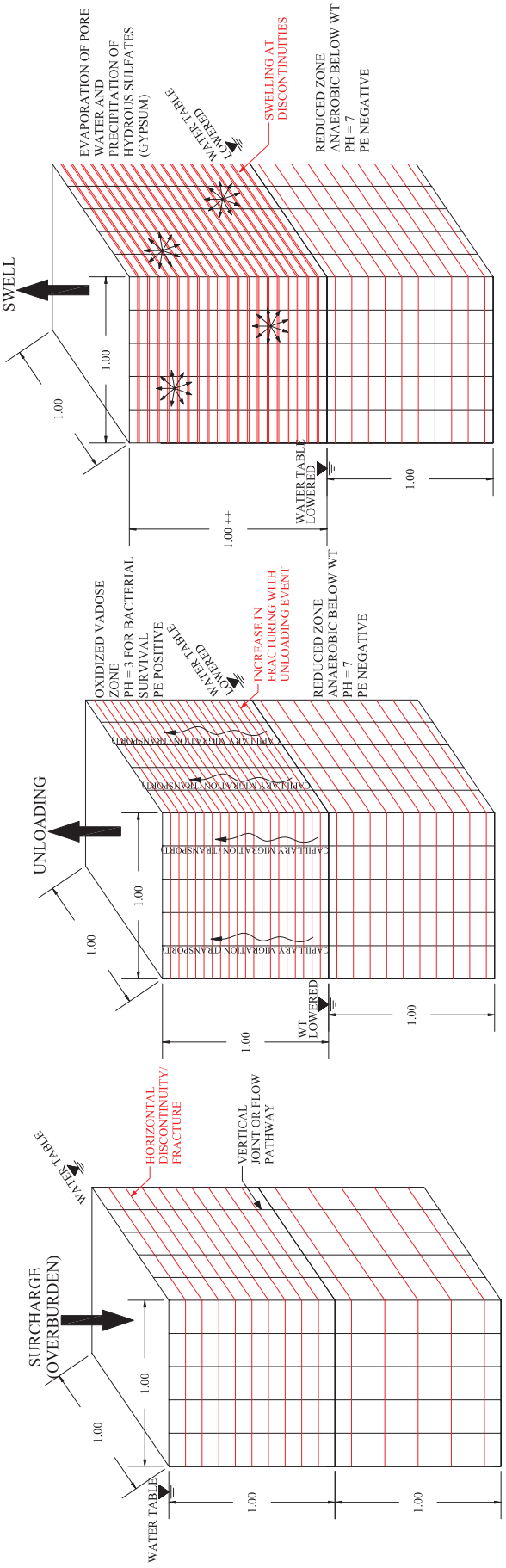

Fig. 1. Expansion associated with pyritic mudstone and hydrous sulphate precipitation is modelled as a stepwise progression during a typical construction project. (**a**) Elevated water table with overburden materials prior to construction. (**b**) Water table is lowered and overburden removed as part of the excavation process, resulting in increased fracturing and oxidation of available pyrite. (**c**) Capillary water evaporates and hydrous sulphates crystallize, resulting in expansion of the mudstone matrix.

capillary rise above a shallow groundwater table (Dougherty & Barsotti 1972; Belgeri & Siegel 1998; Freeman 2003).

This paper will give a broad outline of the chemical and physical nature of expansion in pyritic mudstone and discuss current methods of characterizing their potential for swelling. The samples obtained for this research are from the Devonian Marcellus Shale Formation of North America from various sites in Central Pennsylvania; however, calcareous mudrocks of similar character and with similar concentrations of pyrite and calcium carbonate will probably behave similarly to the Marcellus Shale.

The studies presented in this paper focus on regressive analyses of pyritic mudstone that has undergone significant swelling as a result of gypsum crystallization and has produced heave in overlying structures. This study will provide guidance for determining the potential impacts of pyrite morphology and the complex environmental factors that control the expansive process. The conclusions of this study should aid investigators in identification of potential bedrock conditions that may lead to significant ground heave and provide a direction for future research into this phenomenon.

Observational data

The current method, in the USA, for determining whether shale is potentially expansive involves a chemical analysis of the material to quantify the amount of pyritic sulphur by a recognized laboratory testing method. The ASTM–EPA method outlined in the Pennsylvania DER (1988) Overburden Sampling and Testing Manual is typically utilized in Pennsylvania to determine pyritic sulphur content in shale; however, the acceptable precision of 0.10% pyritic sulphur (S_2) by weight for this test is equal to previously defined thresholds for characterizing the potentially expansive nature of a bedrock formation (Dougherty & Barsotti 1972; Freeman 2003). The ASTM–EPA method measures pyritic sulphur by calculating the difference between total sulphur, which is determined by a combustion method, and the acid-soluble sulphur.

The key question for this prediction model of mudstone expansion is whether the pyrite within the mudstone is sufficiently available for oxidation, reaction with calcite and finally conversion to gypsum. Concentrated deposits of pyrite within fractures, burrows and/or nodules may not have been included as part of the ASTM-EPA method laboratory testing process. The heterogeneity of a particular unit of carbonaceous mudstone and of exposed pyrite and calcite within the mudstone are factors that need to be considered for theoretical and predictive models.

Devonian black mudstones contain a wide variety of diagenetic pyrite morphologies, including disseminated

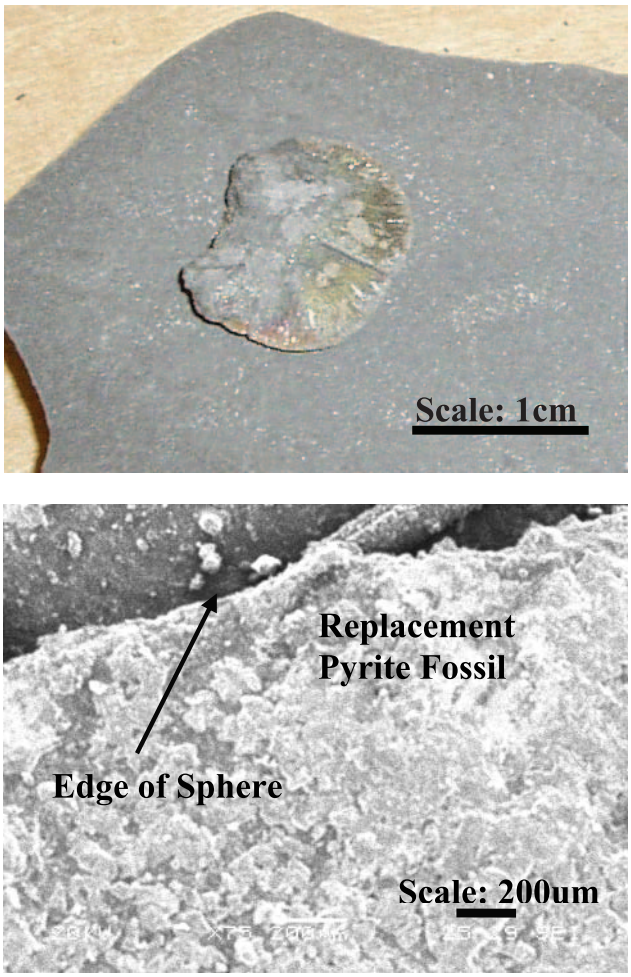

Fig. 2. Replacement pyrite fossil encountered in the Marcellus Shale Formation in Lewisburg, PA. (**a**) Digital photograph of large spheroidal replacement fossil. (**b**) SEM secondary electron (SE) image of same pyrite fossil.

fine crystalline pyrite, framboids, concretions, and sand-sized pyritic spheres. Higher concentrations of macroscopic pyrite, such as *Tazmanites* cysts (Schieber & Baird 2001), can produce highly acidic microenvironments within discontinuities that are conducive to expansion through the precipitation of sulphates. An example of one of these spheres is presented in Figure 2a as a digital photograph and in Figure 2b as an SEM image (Hoover 2002).

The replacement pyrite fossil shown in Figure 2a and b was present within an unoxidized and unweathered zone beneath a floor slab that was damaged by swelling mudstone. Evidence of fully oxidized replacement fossils or 'ghost' pyrite was abundant throughout the zone of swelling. Examples of these fully oxidized portions of the mudstone are shown in Figures 3 and 4.

The observed presence of highly concentrated pyrite zones (see Fig. 2), evidence of full oxidation of these zones (see Fig. 3) and subsequent evidence of abundant gypsum crystal formation (see Fig. 4) suggest that it is the presence of the early diagenetic pyrite that is a key diagnostic feature for identifying the potential for

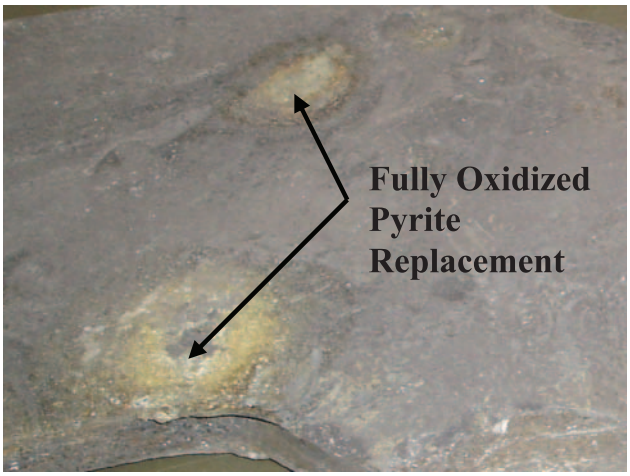

Fig. 3. Digital photograph of fully oxidized zones of pyrite replacement along bedding plane of mudstone beneath floor slab at Evangelical Hospital in Lewisburg, PA.

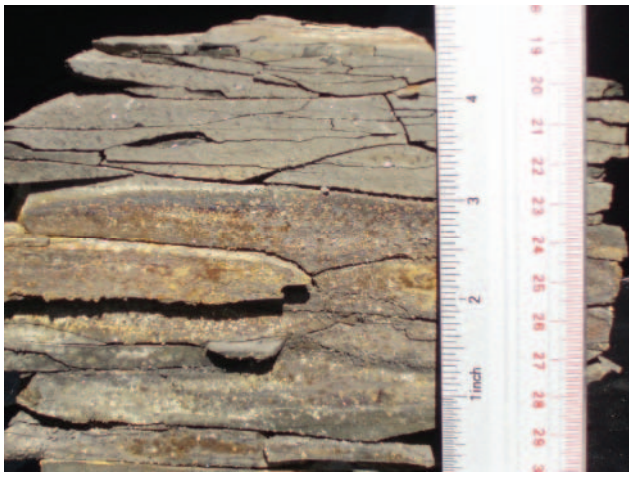

Fig. 4. Digital photograph of a joint cross-section in swelled pyritic mudstone beneath heaved section of floor slab at Evangelical Hospital in Lewisburg, PA.

expansion of mudstone as a result of pyrite oxidation and precipitation of hydrous sulphates.

Figure 5 presents a theorized concentrated pyritic mudstone oxidation–expansion model of the progression of the oxidation process that leads to expansion.

Regressive analysis data

The public domain program Image J, developed by the National Institutes of Health, was utilized in the analysis of thin sections of swelled pyritic mudstone (see Fig. 4). This analysis reveals the presence of distinct gypsum infilling in discontinuities within mudstone fragments. Three thin sections were taken from a single piece of mudstone recovered from beneath a floor slab area that has heaved *c.* 96 mm. The shale contains abundant crystalline gypsum in very fine fractures. The thin sections prepared consist of designations S1 (saw cut perpendicular to joint and bedding plane; PSSC), S2 (saw cut parallel to joint and perpendicular to bedding plane; PSJ) and S3 (saw cut parallel to bedding plane; PSP).

Three sections (left–middle–right) were spatially characterized for each S1 and S2 sample to obtain the quantitative data. A total of 220 and 224 measurements were taken for samples S1 and S2, respectively. Specifically, the distance between gypsum infilling was measured along the entire depth of the sample at three separate cross-sections. Figures 6 and 7 show the examples of the Image J analysis.

The Image J analysis was completed on an optic microscope at $\times 5$ power. Measurements of the distance between the gypsum-filled fractures and the thickness of the infill were used to determine the amount of gypsum present within the sample and percentage swell. This model assumes that there was no gypsum present in the sample prior to oxidation of the pyrite. Table 1 presents the average values for each of the measurements.

These quantitative data were utilized to calculate the amount of pyrite required to produce the calculated amount of gypsum infilling present within the sample. The data obtained from sample S2 were utilized in the regression analysis. It should be notedthat the average swell calculated from this mudstone fragment is higher than the estimated 15.7% overall swell at the area where the sample was extracted. Specifically, *c.* 9.6 cm of surficial heave was measured across an oxidation depth of 61 cm (Hoover & Pease 2007). As is the case in this study, the swell within the single fragments is greater than the global swelling percentage of the oxidized zone. The input parameters for the model are shown in Table 2.

Using the input parameters from Table 2 and the relevant atomic mass data, simple stoichiometry was implemented to determine the theoretical quantity of sulphide sulphur to produce the measured heave in this closed system. The following chemical reaction equations were utilized in the regression analysis:

$$CaCO_3 + H_2SO_4 + 2H_2O \rightarrow CaSO_4 \,.\, 2H_2O + CO_2 + H_2O \quad (1)$$

$$4FeS_2 + 15O_2 + 14H_2O \rightarrow 4Fe(OH)_3 + 8H_2SO_4. \quad (2)$$

Equation 1 describes the reaction of calcite ($CaCO_3$) with sulphuric acid (H_2SO_4) to produce gypsum ($CaSO_4.2H_2O$). It should be noted that the release of carbon dioxide in equation (1) may not be indicative of *in situ* conditions. Equation (2) describes the oxidation of pyrite (FeS_2) with air and water and the subsequent production of sulphuric acid (H_2SO_4) and iron hydroxide ($Fe(OH)_3$, referred to as limonite or 'yellow boy'. These equations do not encapsulate the highly complex oxidation and mineral precipitation processes associated with pyritic materials.

The cell model is a regressive view of the swelling process in expansive pyritic mudstone that is intended to

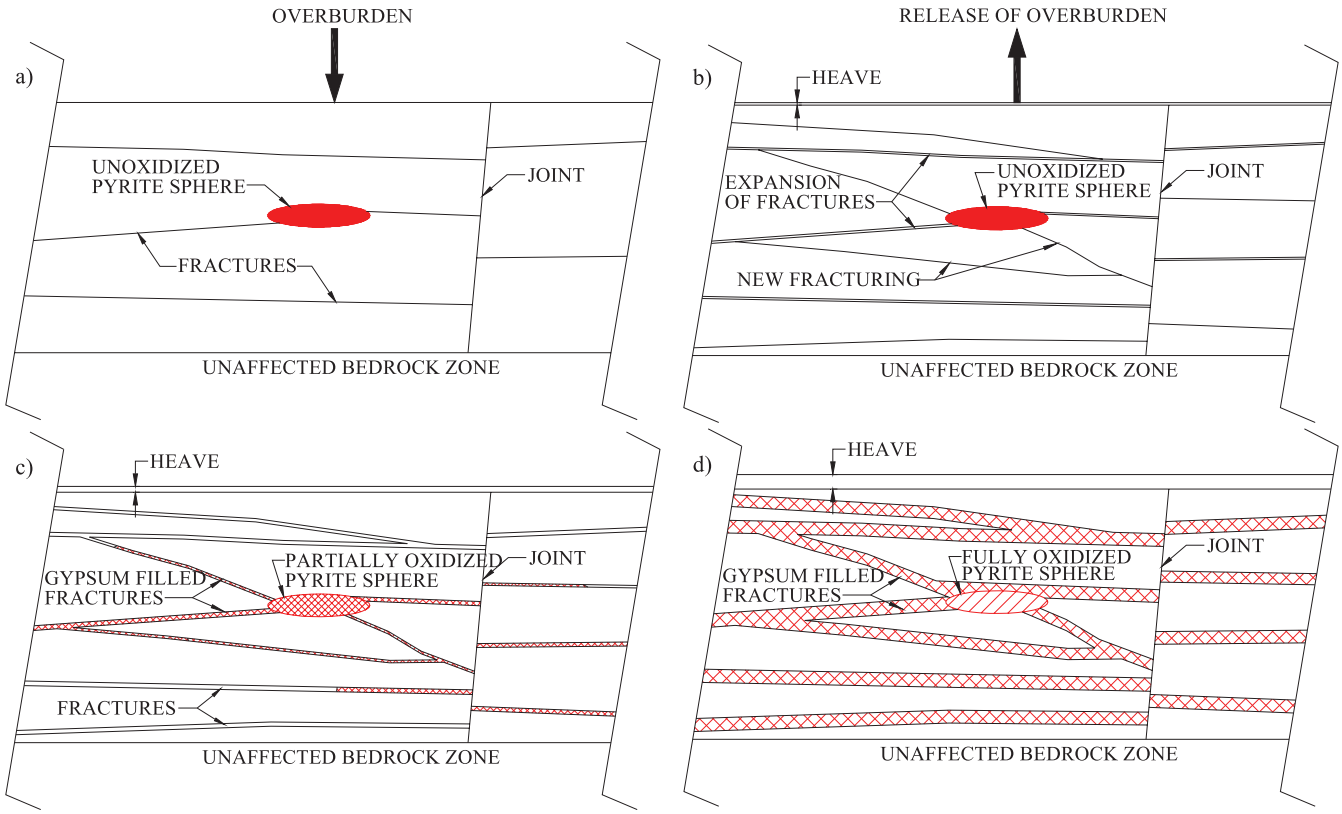

Fig. 5. Theorized concentrated pyritic mudstone oxidation–expansion model. (**a**) Presence of replacement pyrite fossil within calcareous shale under overburden pressure. (**b**) Overburden materials are removed, which induces stress relief fracturing and/or mechanical fracturing in the upper zone and initiation of pyrite oxidation. (**c**) Pyrite oxidation produces sulphuric acid migration through fractures, resulting in the formation of gypsum. Expansion of the fractures through gypsum formation begins to heave overlying structure. (**d**) Pyrite is fully oxidized, resulting in complete infilling of gypsum within the fractures, and swelling is terminated.

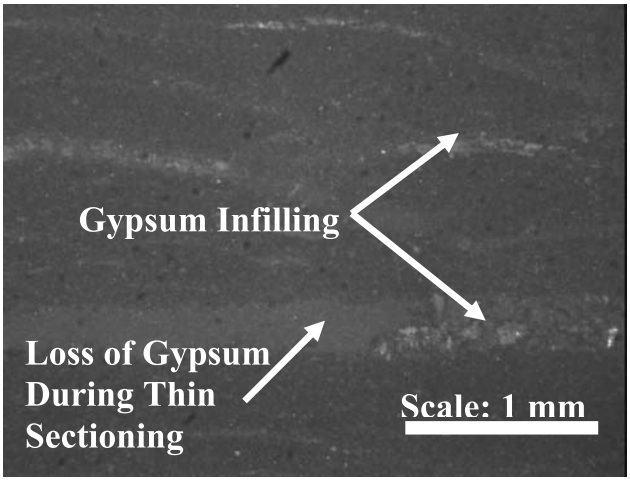

Fig. 6. Image S1M-6; thin section of saw cut perpendicular to joint and bedding plane (PSSC).

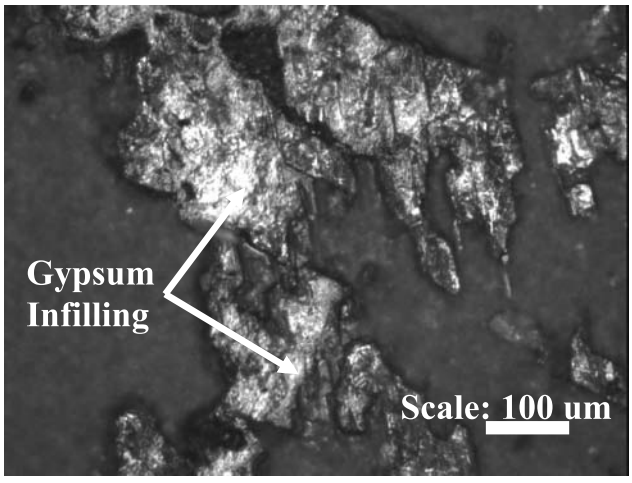

Fig. 7. Image SL3-20; thin section of saw cut parallel to bedding plane (PSP).

determine the possible geochemical and physical mechanisms involved. The input parameters in the model are based on known physical data, which are entered into the regressive stoichiometry of acid generation through oxidation of pyrite. The cell model reveals a total volume of 7.45 cm^3, a gypsum volume of 1.84 cm^3 and a total gypsum mass of 4.23 g.

Stoichiometric calculations reveal a value of 5.36% pyritic sulphur by weight required to produce the amount of gypsum measured. The pyritic sulphur measured in the unoxidized zone beneath the area where the samples were taken measured between 2.5% and 3.5% by weight (Hoover & Pease 2007). It should be noted that the 5.36% pyritic sulphur required to produce

Table 1. *Image J analysis of samples S1 and S2*

Sample	Average section thickness (mm)	Average total thickness of gypsum (mm)	Average swell (%)
S1	16.412	4.630	39.742
S2	19.503	4.821	33.115

Table 2. *Input parameters for regression analysis*

Density of mudstone block	2.7 g cm^{-3}
Density of gypsum	2.3 g cm^{-3}
Number of fractures for reaction availability (N)	10
Dimensions of mudstone cube after heave (x_2)	1.953 cm
Total volume of mudstone cube after heave ($V_2 = x_2^3$)	7.449 cm^3
Average height of gypsum infilling (H)	0.0482 cm
Original height of mudstone block ($x_1 = x_2 - HN$)	1.471 cm
Total initial volume before heave ($V_1 = x_2^2 x_1$)	5.610 cm^3

this heave is the amount that must be available for the reaction within this closed system.

The PHREEQC hydrogeochemical transport model is presented in the Appendix to provide additional support to the conclusions drawn from this simplified cell model.

Conclusions

These values show that concentrated pyritic zones must be available for oxidation to produce the amount of gypsum occurring in fractures below areas of significant structural heave. In this case, the regression analysis shows that the concentration of pyrite required to produce the gypsum infilling (heave) is greater than the amount available within the mudstone fragments; therefore, concentrated pyritic sources outside the closed system must be available for oxidation. Although this model is a very simplified exercise for an extremely complex phenomenon, it does give some idea of the likely dynamics of pyritic mudstone swelling. If shale bedrock contains only around 0.1% pyritic sulphur, the simple stoichiometry does not allow for significant expansion and hydrous sulphate precipitation. Transport or dissolution of gypsum in areas containing low pyritic sulphur contents may be a source of misdiagnosis. Our results show that localized higher concentrations of pyrite within the mudstone fractures, microfractures and macro-voids can be responsible for the expansion, and that the documented cases involving lower pyritic sulphur values may be related to the problems of testing constraints and sampling processes. The higher concentrations of pyrite can be easily overlooked unless the rock is meticulously scanned by an experienced engineering geologist or geotechnical engineer.

These data suggest that a new approach for characterizing the potential for pyritic shales to swell is required. Forms of sulphur testing cannot be utilized as the sole means of characterizing the potential for shales to swell. The precision of the test is questionable and it does not account for all of the factors necessary in analysing the expansive potential for pyritic shales. The experience with the results reported here suggests that a more petrographic approach to analysing rock cores from test borings and samples from test pits is a logical first step. Also, the number of test borings and test pits at a potential building site should be increased, to give a better probability of intersecting areas of shale containing higher concentrations of early diagenetic pyrite (BOCA 1993). The amount of calcium carbonate in the samples is an important factor in the determination of the potential for gypsum growth. Other factors, such as the presence of a water table, amount of overburden and type of structure, are also important in the investigation process. Simple stoichiometry can be applied to estimate the maximum potential heave once the amount and distribution of the pyrite and calcium carbonate are known.

Appendix: PHREEQC hydrogeochemical transport model

PHREEQC (Parkhurst & Appelo 1999) can be utilized to model the various aspects of the processes involved in expansive pyritic mudstone; however, a comprehensive model written entirely in PHREEQC is at present out of reach. An irreversible reaction model can be formulated to simulate the oxidation of pyrite with oxygen at various concentrations of calcite and pyrite and subsequent precipitation of gypsum.

Irreversible reaction

Oxygen and halite are added at a 2:1 ratio and pyrite, calcite, goethite and illite are allowed to dissolve to equilibrium and gypsum is allowed to precipitate if it becomes supersaturated. The CO_2(g) partial pressure has been increased to -2.5 to simulate a semi-closed environment. The first and second runs represent typical amounts of pyritic sulphur that are thought to be present in potentially expansive mudstone (Bryant 2003). Specifically, 0.1% and 0.5% by weight pyritic sulphur contents are modelled in runs one and two, respectively. The third run, consisting of *c.* 1% pyritic sulphur content by weight, considers the effects of more concentrated sources of pyrite available for oxidation within mudstone bedrock. All runs considered 5% $CaCO_3$_ by weight available for reaction.

The model considers a cubic block of mudstone measuring 34 cm × 34 cm × 34 cm with 20 fractures or sites of availability for reaction. There is 1.619 cm spacing between fractures, which is reasonable based on field observations (Hoover & Pease 2007). The final result of the modelling is a change in volume of the cell

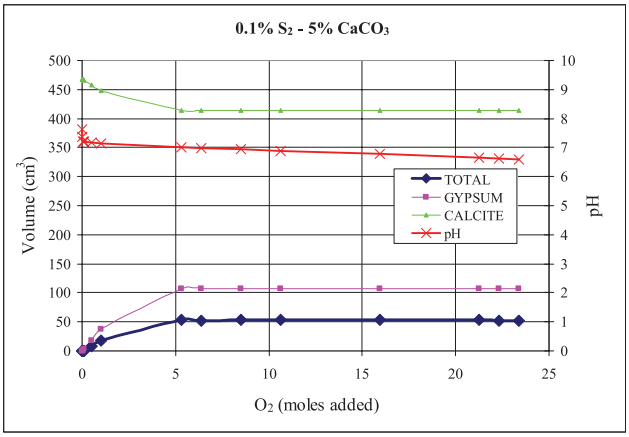

Fig. 8. PHREEQC volume change model at 0.1% S_2 and 5% $CaCO_3$.

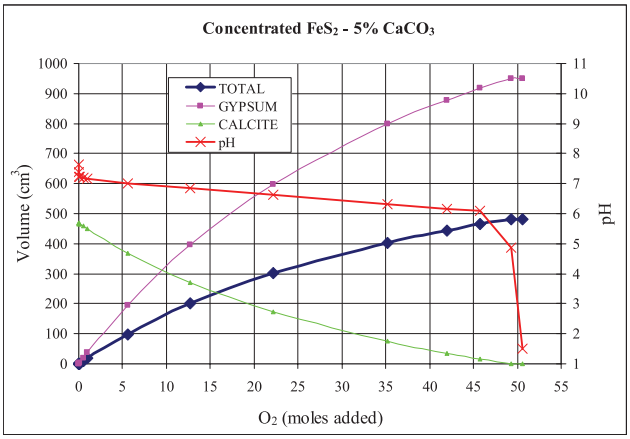

Fig. 10. PHREEQC volume change model at 1.0% S_2 and 5% $CaCO_3$.

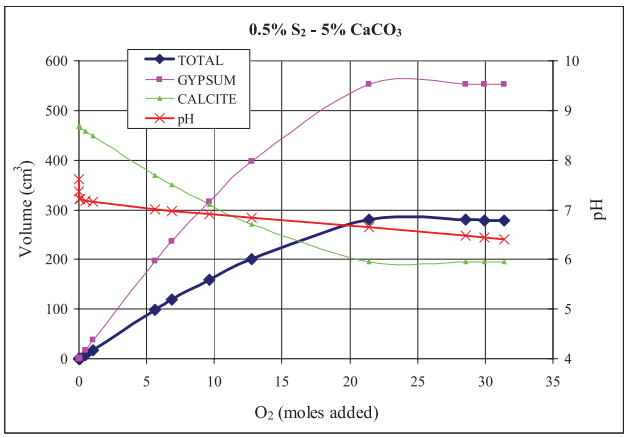

Fig. 9. PHREEQC volume change model at 0.5% S_2 and 5% $CaCO_3$.

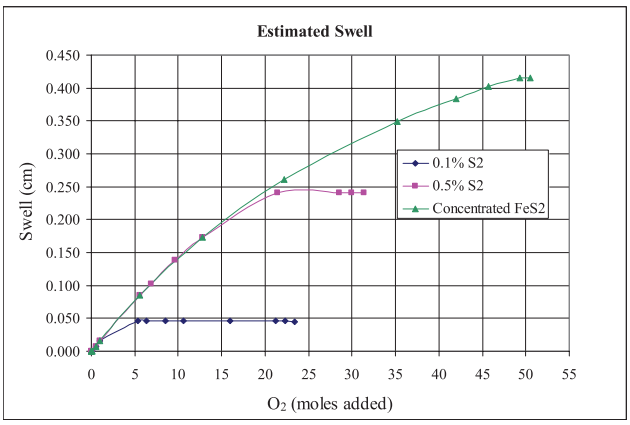

Fig. 11. PHREEQC swelling prediction estimates.

and expansion or elongation in the vertical direction given that the model is constrained from moving in the *x* and *y* directions. This assumption is considered to be a conservative approach, as the main concern for swell is in the vertical direction.

Figures 8–10 represent the total, gypsum and calcite volume change as well as change in pH during the oxidation process at the various percentages of pyritic sulphur. The results indicate that gypsum precipitates and pH stays near seven as long as calcite is in the sample. The pH drops radically as the calcite dissolves out of the system and pyrite continues to oxidize. The Fe^{3+} concentration increases dramatically as the system becomes more acidic and the ferric iron can dissolve and continue to oxidize the pyrite.

The swell model, which considers calcite dissolution and gypsum precipitation, predicts the varying amounts of swelling as shown in Figure 11. The swell model considers the total volume change associated with the dissolution of calcite and precipitation of gypsum. The molar volume difference in these minerals results in a total volume change. The loss of pyrite was not considered in the change in volume calculations for the 0.1% and 0.5% S_2 scenarios because of the potential for a 'honeycombing effect' and given that precipitation of other minerals such as jarosite would probably fill the micro-voids within zones of availability. The 'honeycombing effect' suggests that there would not be a collapse of voids left behind from the dissolution of pyrite and that gypsum would not be replaced with void space upon crystallization. Given the high density of pyrite in comparison with the other minerals in the reaction, the resulting change in volume would not be significant. Also, for the concentrated FeS_2 model, it was assumed that the source of the FeS_2 was within nodules and that an oxidation front would move out from these areas to produce volume change. The swell estimates shown in Figure 11 consider that the *x* and *y* directions of the cell are fixed and that the change in volume corresponds directly to a change in height.

The estimated swell amounts shown in Figure 11 are based on the total volume change predictions presented in Figures 8–10 with the assumption that the swell is a function of the cell dimensions of monoclinic gypsum crystals (least dimension representing the change in the vertical direction).

The example run in PHREEQC broadly describes some of the geochemical processes that occur in expansive pyritic mudstone. PHREEQC may be utilized to develop

a model that shows a contribution of the example presented in this paper; however, this program will not be able to explain the mechanics involved in the creation of sulphate precipitation and subsequent expansion.

An interesting correlation can be made between the results of the regression analysis and the PHREEQC analysis. The third PHREEQC run models a high concentration of pyrite that would be similar to the presence of pyritic nodules or replacement pyrite fossils. Specifically, there are 6.420 moles of pyrite and 12.705 moles of calcite in the PHREEQC model producing the greatest heave, which gives a calcite to pyrite mole ratio of 1.98. The regression model presented calculates 0.012 moles of pyrite and 0.025 moles of calcite, which gives a calcite to pyrite mole ratio of 2.08. It should be noted that this does not assume that all available pyrite and calcite are completely consumed, which suggests that additional precipitation of gypsum would be possible. The agreement in mole ratio between two very different models is very compelling support for the microenvironmental theory and the importance of highly concentrated sources of pyrite in the Devonian Marcellus Shale Formation.

Acknowledgements. This research was conducted at the Pennsylvania State University and Juniata College as part of S.E.H.'s doctoral thesis.

References

Anon. 1960. Structures don't settle in this shale, but watch out for heave. *Engineering News Record*, **164**, 46–48.

Appelo, C.A.J. & Postma, D. 1993. *Geochemistry, Groundwater and Pollution*. Balkema, Rotterdam.

Belgeri, J.J. & Siegel, T.C. 1998. Design and performance of foundations in expansive shale. *Ohio River Valley Soils Seminar XXIV, Louisville, KY*, 2–6.

Bell, F.G. 2000. *Engineering Properties of Soils and Rock*, 4th edn. Blackwell Science, Oxford, 277–281.

Building Officals Code Administrators International, Inc. (BOCA) 1993. *The BOCA National Building Code. Presumptive Load Bearing Values of Foundation Materials*. Chicago, K.

Brady, K.B.C., Smith, M.W. & Schueck, J. (eds) 1998. *Coal Mine Drainage Prediction and Pollution Prevention in Pennsylvania*. Pennsylvania Department of Environmental Protection, Harrisburg, PA.

Bryant, L.D. 2003. *Geotechnical problems with pyritic rock and soil*. MSc Thesis, Virginia Polytechnic Institute and State University, Blacksburg, VA.

Coveney, R.M. & Parizek, E.J. 1977. Deformation of mine floor by sulfide alteration. *Bulletin of Association of Engineering Geologists*, **XIV**, 131–156.

Dougherty, M.T. & Barsotti, N.J. 1972. Structural damage and potentially expansive sulfide minerals. *Bulletin of the Association of Engineering Geologists*, **IX**, 105–125.

Dubbe, D.E., Usmen, M.A. & Moulten, L.K. 1984. *Expansive Pyritic Shales*. Transportation Research Board, Washington, DC.

Freeman, T.E. 2003. *Final Report—Forensic Investigation of Pavement Distress: Old Airport Road in Bristol, Virginia*. Virginia Transportation Research Council, Charlottesville, VA.

Gold, D.P. & Doden, A.G. 2006. *The Age, Depth, and Nature of Acid-Generating Mineralization along Segments of I-99 on Bald Eagle Ridge*. Pennsylvania Department of Transportation Bureau of Planning and Research, Harrisburg, PA.

Hammarstrom, J.M., Seal, R.R. II, Meir, A.L. & Kornfield, J.M. 2004. Secondary sulfate minerals associated with acid drainage in the eastern U.S.: recycling of metals and acidity in surficial environments. *Chemical Geology*, **215**, 407–431.

Hawkins, A.B. & Pinches, G.M. 1987. Cause and significance of heave at Llandough Hospital, Cardiff—a case history of ground heave due to gypsum growth. *Quarterly Journal of Engineering Geology*, **20**, 41–57.

Hoover, S.E. & Pease, J.B. 2007. Micropile underpinning over expansive pyritic shales. *Eighth International Workshop on Micropiles, Toronto, Ont*, 5–6.

Hoover, S.E., Dempsey, B.A. & Wang, M.C. 2004. Structural damage induced by pyritic shale. *Fifth International Conference on Case Histories in Geotechnical Engineering, New York*, 1–6.

Jangdal, C.E. 1971. Swelling shale in the Ostersund area. *National Swedish Building Research*, **R35**, 116.

Jaynes, D.B, Pionke, H.B. & Rogowski, A.S. 1984*a*. Acid mine drainage from reclaimed coal strip mines—2. Simulation results of model. *Water Resources Research*, **20**, 243–250.

Jaynes, D.B., Rogowski, A.S. & Pionke, H.B. 1984*b*. Acid mine drainage from reclaimed coal strip mines—1. Model description. *Water Resources Research*, **20**, 233–242.

Long, J.D. & Williams, P.A. 1990. *Report of Structural Distress Investigation—Phase I, Johnson City Public Library*. S&ME, Blountville, TN.

Moum, J. & Rosenqvist, I. 1959. Sulfate attack on concrete in the Oslo region. *Journal of the American Concrete Institute*, **56**, 257–264.

Parkhurst, D.L. & Appelo, C.A.J. 1999. *User's guide to PHREEQC (Version 2)—a computer program for speciation, batch-reaction, one-dimensional transport, and inverse geochemical calculations*. US Geological Survey Water-Resources Investigations Report, **99-4259**.

Penner, E. & Eden, W.J. 1972. *Expansion of Pyritic Shales*, Canadian Building Digest, **CBD-152**. National Research Council Canada, Ottawa, ON. World Wide Web Address: www.nrc.ca/irc/cbd/cbd152e.html.

Pennsylvania Department of Environmental Resources. 1988. *Overburden Sampling and Testing Manual*. Small Operator Assistance Program, Bureau of Mining and Reclamation, Harrisburg, PA.

Rimstidt, J.D. & Newcomb, W.D. 1993. Measurement and analysis of rate data—the rate of reaction of ferric iron with pyrite. *Geochimica et Cosmochimica Acta*, **57**, 1919–1934.

Schieber, J. & Baird, G. 2001. On the origin and significance of pyrite spheres in Devonian black shales, North America. *Journal of Sedimentary Research*, **71**, 155–166.

Tanguay, C., Perrier, Y. & Hebert, F.1999. *Pyrite and Your House*. Association des Consommateurs pour la Qualité dans la Construction, Montreal, Que.

Received 17 December 2007; accepted 20 October 2008.